Thermo, pH and reduction responsive coaggregates comprising AB2C2 star terpolymers for multi-triggered release of doxorubicin

Journal:	*Polymer Chemistry*
Manuscript ID:	PY-ART-12-2013-001767.R1
Article Type:	Paper
Date Submitted by the Author:	29-Jan-2014
Complete List of Authors:	Zhao, Youliang; Soochow University, College of Chemistry, Chemical Engineering and Materials Science Miao, Ke; Soochow University, Liu, Huanhuan; Soochow University,

Journal Name

Cite this: DOI: 10.1039/c0xx00000x

www.rsc.org/xxxxxx

ARTICLE TYPE

Thermo, pH and reduction responsive coaggregates comprising AB_2C_2 star terpolymers for multi-triggered release of doxorubicin†

Ke Miao, Huanhuan Liu and Youliang Zhao*

Received (in XXX, XXX) Xth XXXXXXXXX 20XX, Accepted Xth XXXXXXXXX 20XX

DOI: 10.1039/b000000x

Novel 5-arm $PEG(PCL)_2(PNIPAM)_2$ (S1) and $PEG(PCL)_2(PAA)_2$ (S3) star terpolymers were synthesized, and their aggregates formed by a single star or mixed stars were efficiently used for loading and release of doxorubicin upon dual and triple stimuli. The star terpolymers had two disulfide moieties and poly(ethylene glycol) (PEG, A), poly(ε-caprolactone) (PCL, B), poly(*N*-isopropylacrylamide) (PNIPAM, C_1), poly(*tert*-butyl acrylate) (P*t*BA, C_2), and poly(acrylic acid) (PAA, C_3) segments. Terminal diazide functionalized PEG ($PEG\text{-}(N_3)_2$) and alkyne-mid-functionalized PCL-*b*-PNIPAM and PCL-*b*-P*t*BA diblock copolymers were subjected to azide-alkyne cycloaddition reaction to generate AB_2C_2 (C = C_1 and C_2) stars, and followed by selective hydrolysis to obtain $PEG(PCL)_2(PAA)_2$ star. Polymeric micelles were prepared by self-assembly of a single star in aqueous solution, and coaggregates were obtained by coassembly of S1 and S3 mixtures. Various polymeric aggregates had a great potential as controlled delivery vehicles due to their reasonable drug loading efficiency and stimuli-adjustable drug release properties. As compared with dually sensitive micelles formed from a single star, triply stimuli-responsive coaggregates may be more promising as controlled delivery vehicles since the drug release properties can be potentially adjusted by various external stimuli and composition of star mixtures.

Polymeric aggregates have been extensively investigated for their great potential applications in biomedical materials.[1–18] The self-assembled systems can solubilize hydrophobic drugs, avoid non-selective uptake by the reticuloendothelial system, and utilize the enhanced permeability and retention effect for passive targeting. Tremendous progress in polymer science enables facile construction of stimuli-responsive polymeric aggregates as versatile nanocarriers for drug delivery.[19–30] Among families of functional polymers, pH-sensitive poly(acrylic acid) (PAA) and thermo-responsive poly(*N*-isopropylacrylamide) (PNIPAM) belong to representative smart segments, and biodegradable poly(ε-caprolactone) (PCL) and biocompatible poly(ethylene glycol) (PEG) are widely used in biomedical materials due to their excellent physicochemical and biological properties. Thus far, many stimuli-sensitive copolymer aggregates bearing these functional segments have been developed for smart release systems, and the introduction of cleavable linkages can further endow aggregates with tunable functionalities and parameters. Upon internal or external stimuli, the drug-loaded aggregates can perform the dissociation or morphology changes, and thus the release process can be further accelerated.

Generally speaking, normal polymeric aggregates formed from a single polymer can be efficiently used to construct the ordered micelles or vesicles via self-assembly;[31–34] however, they suffer from lack of multiple functionalities in some cases due to the limitation in the number of building blocks. To further address this limitation, the construction of multifunctional mixed aggregates with two or more kinds of polymers via coassembly has been developed.[35–44] This straightforward strategy has some advantages such as wider availability of tailored block copolymers, easier control over micellar properties via altering chemical composition and weight ratio of various polymers, and more facile attachment of functional molecules via versatile postmodification reactions. At present, it is of great importance to extend this approach to construct multifunctional systems with potential applications in functional materials and nanotechnology.

Although a large number of mixed aggregates have been achieved to be superior to their individual constituents,[35–44] little attention has been paid to stimuli-responsive coaggregates based on multicomponent star copolymers. These complex architectures usually exhibit smaller hydrodynamic radius, lower intrinsic viscosity and denser functional groups as compared with their linear analogues with similar composition and molecular weight. Moreover, miktoarm stars comprising different arm segments can undergo microphase separation at molecular level and self-assemble into intriguing supramolecular assemblies involving multicompartment micelles originating from their branched architectures and heterophase structures.[45–55] Owing to their special microphase separation behaviors, star copolymer aggregates usually exhibited more controllable drug release behaviors than those formed by their linear counterparts.[56–66] Therefore, star copolymers are expected to better meet various requirements and optimize the properties of multifunctional aggregates. However, smart drug delivery systems based on multicomponent star copolymers with cleavable moieties are relatively scarce thus far.

Herein we reported on facile construction of mixed aggregates based on disulfide-linked AB_2C_2 (A = PEG, B = PCL, and C = PNIPAM or PAA) star terpolymers for multiple stimuli-triggered drug release. Terminal diazide functionalized PEG ($PEG\text{-}(N_3)_2$)

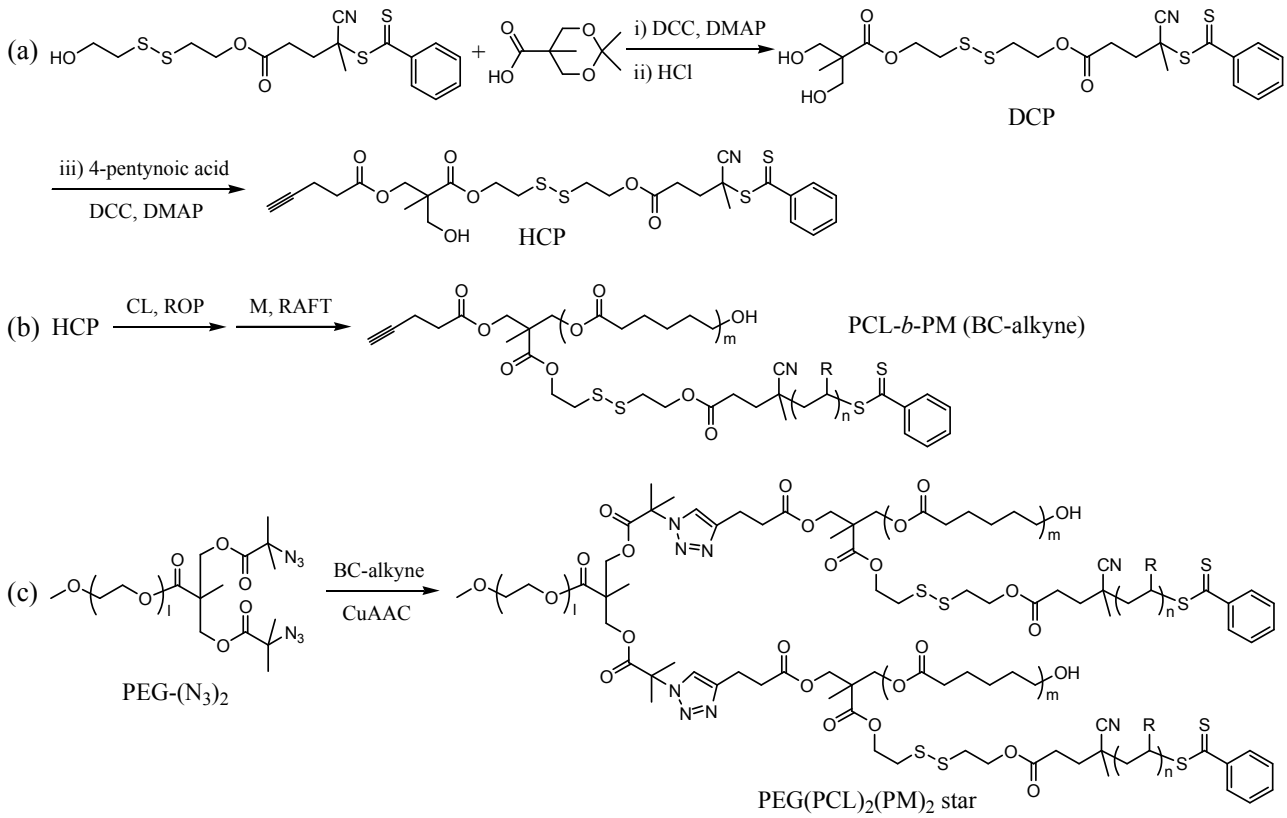

Scheme 1 Synthetic routes to two-disulfide-functionalized 5-arm $PEG(PCL)_2(PNIPAM)_2$ (R = $CONHCH(CH_3)_2$, S1), $PEG(PCL)_2(PtBA)_2$ (R = $COOC(CH_3)_3$, S2), and $PEG(PCL)_2(PAA)_2$ (R = COOH, S3, which was obtained by hydrolysis of S2 using CF_3COOH) star terpolymers by combination of ROP, RAFT process and CuAAC.

and excess alkyne-mid-functionalized PCL-*b*-PNIPAM or PCL-*b*-P*t*BA were subjected to copper(I)-catalyzed azide-alkyne cycloaddition (CuAAC) reaction[67] to generate 5-arm $PEG(PCL)_2(PNIPAM)_2$ (S1) and $PEG(PCL)_2(PtBA)_2$ (S2) star copolymers, and $PEG(PCL)_2(PAA)_2$ star (S3) was obtained by selective hydrolysis of S2 to convert poly(*tert*-butyl acrylate) (P*t*BA) into PAA segment (Scheme 1). The resultant star terpolymers and their precursors were characterized by ^1H NMR, GPC-MALLS, and IR. Moreover, their self-assembly behaviors, and stimuli-triggered drug loading and release properties were investigated.

The novelty of this study primarily lies in three aspects. First, two examples of novel AB_2C_2-type star terpolymers with sensitive PNIPAM or PAA segments were synthesized by combination of ROP, RAFT process and CuAAC, in which the introduction of disulfide linkages renders reduction responsiveness of copolymer aggregates. Second, drug loading and release from copolymer aggregates formed from a single star and star copolymer mixtures were investigated, and dually and triply sensitive release systems were constructed via (co)aggregation. Last, this study can not only promote further understanding of structure-property relationship of cleavable multicomponent star copolymers but extend their potential applications, in which the thermo-, pH- and reduction-sensitive coaggregates involving four components were used as versatile nanocarriers for smart drug delivery, and the special function of each segment could be integrated into multifunctional coaggregates. To the best of our knowledge, our study is the first report on coassembly and drug delivery system based on novel AB_2C_2 star terpolymers. The success of this study further paves ways for facile construction of multiply sensitive smart drug delivery systems.

Experimental section

Materials

All solvents, monomers, and other chemicals were purchased from Sigma-Aldrich unless otherwise stated. *N*-Isopropylacrylamide (NIPAM, 97%) was recrystallized twice from mixtures of hexane and toluene, *tert*-butyl acrylate (*t*BA, 98%) was passed through a basic alumina column to remove the inhibitor, and ε-caprolactone (CL, 99%) was distilled from calcium hydride under reduced pressure. Bis(2-hydroxyethyl) disulfide (Alfa Aesar, 90%) was distilled under reduced pressure, dichloromethane (DCM) and dioxane were dried and distilled over CaH_2, toluene was distilled over sodium and benzophenone, and *N*,*N*-dimethylformamide (DMF) was dried over $MgSO_4$ and distilled under reduced pressure. 2,2′-Azobis(isobutyronitrile) (AIBN) was recrystallized twice from ethanol. *N*,*N*′-Dicyclohexylcarbodiimide (DCC) and 4-dimethylamino pyridine (DMAP) were purchased from Sinopharm Chemical Reagent Co., Ltd. and used as received. CuBr (98%) was purified by stirring in

acetic acid and washing with ethanol and then dried in vacuo. Stannous octoate ($Sn(Oct)_2$, 97%), *N,N,N′,N″,N″*-pentamethyldiethylenetriamine (PMDETA, 99%), poly(ethylene glycol) monomethylether (MPEG, M_n = 2000 g mol^{-1}), 2,2-bis(hydroxylmethyl) propionic acid (Bis-HMPA, 98%), 2,2′-dimethoxypropane (98%), sodium azide (99%, Alfa Aesar), D,L-dithiothreitol (DTT, 99%, Merck), and doxorubicin hydrochloride (99%, Zhejiang Hisun Pharmaceutical Co, Ltd.) were used as received. Terminal diazide functionalized PEG (PEG-$(N_3)_2$),[55] 4-cyanopentanoic acid dithiobenzoate (4-CPDB),[68] 2-((2-hydroxy ethyl)disulfanyl)ethyl 4-cyano-4-(phenylcarbonothioylthio) pentanoate,[69] isopropylidene-2,2'-bis(methoxyl)propionic acid,[70] and azide- and alkyne-functionalized silica particles (with loadings of 0.612 mmol g^{-1} for Si-N_3 and 0.398 mmol g^{-1} for Si-alkyne)[71,72] were synthesized and purified according to literature procedures.

Synthesis of DCP

To a round flask were added 2-((2-hydroxyethyl)disulfanyl)ethyl 4-cyano-4-(phenylcarbonothioylthio)pentanoate (7.0 g, 16.8 mmol), isopropylidene-2,2'-bis(methoxyl)propionic acid (3.58 g, 20.0 mmol), DMAP (0.20 g, 1.6 mmol) and 200 mL of dry DCM under nitrogen, and followed by slow addition of a 50 mL of DCM solution comprising DCC (4.12 g, 20.0 mmol) in 1 h. The mixture was further reacted at ambient temperature for 20 h. The crude product was filtered, concentrated and purified by flash column chromatography eluting with ethyl acetate / petroleum ether (1:3, v/v) to give 9.10 g (15.9 mmol, 94.6% yield) of 2-((2-(isopropylidene-2,2'-bis(methoxyl)propionyloxy)ethyl)disulfanyl) ethyl 4-cyano-4-(phenylcarbonothioylthio)pentanoate (ICP).

The resultant ICP was dissolved in 50 mL of THF, and then 50 mL of 1 M HCL was added into the mixture solution. The mixture was stirred at room temperature for 18 h. The mixture was evaporated under reduced pressure and partitioned between water (50 mL) and DCM (200 mL). The organic phase was washed with deionized water (20 mL × 3), collected and dried with $MgSO_4$. After filtration and concentration, 2-((2-((2,2-dihydroxymethyl)propionyloxy)ethyl)disulfanyl)ethyl 4-cyano-4-(phenylcarbonothioylthio)pentanoate (DCP) was isolated in 97.1% yield.

DCP: ^{1}H NMR ($CDCl_3$): δ 7.92, 7.58, 7.41 (m, 5H, Ph*H*), 4.45 (m, 2H, CH_2O), 4.39 (m, 2H, CH_2O), 3.91 and 3.75 (dd, *J* 4.8, 4H, CH_2OH), 2.96 (t, *J* 4.4, 4H, CH_2S), 2.3-2.9 (m, 4H, CH_2CH_2CO), 1.95 (s, 3H, CH_3), 1.08 (s, 3H, CH_3). ^{13}C NMR ($CDCl_3$): δ 222.2 (*C*=S), 175.4, 171.3 (*C*=O), 144.3, 133.0, 128.5, 126.6 (Ph*C*), 118.4 (*C*N), 67.2, 62.7, 62.3, 49.4, 45.6, 36.9, 33.2, 29.6, 24.0, 17.1. IR (KBr): 3417, 3060, 2933, 2887, 2851, 2232, 1732, 1627, 1589, 1445, 1388, 1296, 1226, 1180, 1047, 998, 902, 869, 802, 763, 688 cm^{-1}. Anal. Calcd for $C_{22}H_{29}NO_6S_4$: C, 49.69%; H, 5.50%; N, 2.63%; S, 24.12%. Found: C, 49.32%; H, 5.59%; N, 2.58%; S, 24.01%.

Synthesis of HCP

To a round flask were added DCP (6.02 g, 11.3 mmol), DCC (3.50 g, 16.9 mmol), DMAP (0.13 g, 1.2 mmol) and 250 mL of dry DCM under nitrogen, and followed by slow addition of a 30 mL of DCM solution comprising 4-pentynoic acid (1.11 g, 11.3 mmol) to perform the esterification. The mixture was reacted at room temperature for 18 h, filtered, and concentrated. The crude product was purified by flash column chromatography eluting with ethyl acetate / petroleum ether (1:3, v/v), and 3.77 g (54.6% yield) of 2-((2-((2-hydroxymethyl-2-(pent-4-ynoyloxy)methyl) propionyloxy)ethyl)disulfanyl)ethyl 4-cyano-4-(phenylcarbono thioylthio)pentanoate (HCP) was obtained as a red oil.

HCP: ^{1}H NMR ($CDCl_3$): δ 7.92 (d, *J* 8.0, 2H, Ph*H*), 7.58 (t, *J* 7.2, 1H, Ph*H*), 7.41 (t, *J* 7.6, 2H, Ph*H*), 4.40 and 4.28 (m, 6H, CH_2O), 3.70 (s, 2H, CH_2OH), 2.94 (t, *J* 6.0, 4H, CH_2S), 2.3-2.8 (m, 8H, CH_2CH_2CO), 1.99 (s, 1H, C*H*), 1.95 (s, 3H, CH_3), 1.23 (s, 3H, CH_3). ^{13}C NMR ($CDCl_3$): δ 222.2 (*C*=S), 173.8, 171.6, 171.2 (*C*=O), 144.3, 133.0, 128.5, 126.5 (Ph*C*), 118.3 (*C*N), 82.2 (CH≡*C*), 69.3 (*C*H≡C), 65.7, 64.7, 62.6, 62.3, 48.2, 45.5, 36.8, 33.1, 29.5, 23.9, 17.3, 14.2. IR (KBr): 3452, 3300 (ν_{CH} of alkyne), 3060, 2937, 2887, 2232 ($\nu_{C\equiv N}$), 2119 ($\nu_{C\equiv C}$), 1736 ($\nu_{C=O}$), 1631, 1459, 1445, 1385, 1293, 1232, 1178, 1049, 997, 902, 869, 764, 688 cm^{-1}. Anal. Calcd for $C_{27}H_{33}NO_7S_4$: C, 53.00%; H, 5.44%; N, 2.29%; S, 20.96%. Found: C, 52.66%; H, 5.52%; N, 2.28%; S, 20.79%.

Synthesis of PCL macro chain transfer agent (CTA)

To a Schlenk tube were added HCP (0.500 g, 0.817 mmol), CL (4.66 g, 40.9 mmol), and $Sn(Oct)_2$ (0.067 g, 0.16 mmol) under nitrogen, and toluene was added until the total volume was 13.6 mL. The contents were degassed by three freeze-pump-thaw cycles and polymerized at 90 ^{o}C for 20 h. The polymer was concentrated and precipitated into methanol thrice, and 4.40 g (monomer conversion: 83.7%) of PCL was obtained after vacuum drying. Apparent molecular weight and polydispersity (PDI) estimated by GPC were $M_{n,GPC}$ = 8000 g mol^{-1} and PDI = 1.13, and number-average molecular weight was determined to be $M_{n,NMR}$ = 5600 g mol^{-1} by ^{1}H NMR analysis.

PCL: ^{1}H NMR ($CDCl_3$): δ 7.92 (d, *J* 7.6, Ph*H*), 7.58 (t, *J* 7.6, Ph*H*), 7.41 (t, *J* 7.2, Ph*H*), 4.2-4.5 (m, CH_2O), 4.06 (t, *J* 6.8, CH_2O of PCL), 3.65 (t, *J* 6.8, terminal CH_2OH), 2.92 (t, *J* 5.6, CH_2S), 2.4-2.8 (m, CH_2CH_2COO), 2.31 (t, *J* 7.6, CH_2CO of PCL), 1.99 (s, C*H*≡C), 1.95 (s, CH_3), 1.65 (m, CH_2 of PCL), 1.38 (m, CH_2 of PCL), 1.27 (s, CH_3). FT-IR (KBr): 3440, 2945, 2866, 1731, 1471, 1420, 1396, 1369, 1296, 1244, 1192, 1164, 1106, 1046, 962, 933, 869, 841, 764, 732, 691 cm^{-1}.

Synthesis of alkyne and disulfide functionalized PCL-*b*-PM diblock copolymers

In a typical polymerization, NIPAM (0.509 g, 4.50 mmol), PCL (0.560 g, 0.100 mmol), AIBN (1.6 mg, 0.010 mmol), and 3.3 mL of dioxane were added to a glass tube with a magnetic stirring bar. The tube was sealed with a rubber septum, and the mixture was flushed with nitrogen for 15 min. Subsequently, the tube was immersed into an oil bath thermostated at 70 °C for 18 h. The reaction mixture was concentrated and precipitated in cold diethyl ether thrice, and 0.920 g (monomer conversion: 70.8%) of PCL-*b*-PNIPAM copolymer was obtained. PCL-*b*-P*t*BA copolymer were synthesized and purified according to a similar procedure.

PCL-*b*-PNIPAM: $M_{n,GPC}$ = 11200 g mol^{-1}, PDI = 1.15, and $M_{n,NMR}$ = 9220 g mol^{-1}. ^{1}H NMR ($CDCl_3$): δ 7.96, 7.57, 7.40 (m, Ph*H*), 6.0-7.2 (m, N*H* of PNIPAM), 4.2-4.5 (m, CH_2O), 4.07 (m, CH_2O of PCL and C*H*NH of PNIPAM), 3.65 (t, *J* 6.8, terminal

CH_2OH), 2.92 (t, *J* 5.6, CH_2S), 2.4-2.8 (m, CH_2CH_2COO), 2.31 (t, *J* 7.6, CH_2CO of PCL), 0.6-2.2 (m, C*H*≡C and CH_3 resulting from CTA, CH_2CH and CH_3 of PNIPAM, and CH_2 of PCL). FT-IR (KBr): 3439, 2939, 2868, 1736, 1648, 1545, 1460, 1420, 1387, 1367, 1237, 1164, 1094, 1064, 1043, 967, 879, 734, 690 cm^{-1}.

PCL-*b*-P*t*BA: $M_{n,GPC}$ = 13100 g mol^{-1}, PDI = 1.12, and $M_{n,NMR}$ = 12000 g mol^{-1}. ^1H NMR ($CDCl_3$): δ 7.96, 7.53, 7.37 (m, Ph*H*), 4.2-4.5 (m, CH_2O), 4.06 (t, *J* 6.8, CH_2O of PCL), 3.65 (t, *J* 6.8, terminal CH_2OH), 2.92 (t, *J* 5.6, CH_2S), 2.4-2.6 (m, CH_2CH_2COO), 2.31 (t, *J* 7.2, CH_2CO of PCL), 2.23 (m, CH_2CH of P*t*BA), 0.6-2.1 (m, C*H*≡C and CH_3 resulting from CTA, CH_2 of PCL, and CH_2 and CH_3 of P*t*BA). FT-IR (KBr): 3439, 2938, 2868, 1731, 1637, 1560, 1459, 1394, 1368, 1261, 1150, 1101, 1017, 961, 908, 846, 802, 750, 693 cm^{-1}.

Synthesis of 5-arm PEG(PCL)$_2$(PM)$_2$ miktoarm stars via click reaction between PEG-(N$_3$)$_2$ and PCL-*b*-PM

PEG-$(N_3)_2$ (46.8 mg, 0.020 mmol), PCL-*b*-PNIPAM (0.553 g, 0.060 mmol), and PMDETA (6.9 mg, 0.040 mmol) were dissolved in DMF (6.0 mL) in Schlenk tube. After three freezing-thawing cycles, CuBr (5.8 mg, 0.040 mmol) was added under nitrogen. The tube was subsequently immersed into an oil bath thermostated at 60 °C for 30 h, and then 0.30 g (0.18 mmol of azide functionality) of Si-N_3 and 0.45 g (0.18 mmol) of Si-alkyne were added to the tube under nitrogen. The reaction was further performed at 80 °C for 20 h under vigorous stirring. The mixture was diluted with 30 mL of THF and passed through alumina column. The polymer solution was concentrated under reduced pressure and precipitated into cold methanol. After vacuum drying, 0.353 g (84.8% yield) of PEG$(PCL)_2(PNIPAM)_2$ star terpolymer (S1) was obtained. Number-average molecular weights and polydispersity determined by GPC-MALLS and NMR analyses were $M_{n,LS}$ = 22000 g mol^{-1}, PDI = 1.08, and $M_{n,NMR}$ = 20900 g mol^{-1}. PEG$(PCL)_2$(P*t*BA)$_2$ star (S2) was synthesized and purified according to a similar procedure.

PEG$(PCL)_2(PNIPAM)_2$ star: ^1H NMR ($CDCl_3$): δ 7.96 (m, Ph*H*), 7.54 (m, Ph*H* and C*H* of triazole), 7.40 (m, Ph*H*), 6.0-7.2 (m, N*H* of PNIPAM), 4.2-4.5 (m, CH_2O), 4.06 (m, CH_2O of PCL and C*H*NH of PNIPAM), 3.65 (s, CH_2CH_2O of PEG and terminal CH_2OH of PCL), 3.38 (s, CH_3O), 3.01 (m, CH_2-triazole), 2.92 (s, CH_2S), 2.4-2.8 (m, CH_2CH_2COO), 2.31 (t, *J* 7.6, CH_2CO of PCL), 0.6-2.2 (m, CH_3 resulting from CTA, CH_2CH and CH_3 of PNIPAM, and CH_2 of PCL). FT-IR (KBr): 3440, 2944, 2866, 1725, 1648, 1551, 1471, 1420, 1385, 1368, 1296, 1245, 1192, 1107, 1065, 1045, 961, 933, 841, 732 cm^{-1}.

PEG$(PCL)_2$(PtBA)$_2$ star: ^1H NMR ($CDCl_3$): δ 7.94 (m, Ph*H*), 7.55 (m, Ph*H* and C*H* of triazole), 7.44 (m, Ph*H*), 4.2-4.5 (m, CH_2O), 4.06 (m, CH_2O of PCL), 3.65 (s, CH_2CH_2O of PEG and terminal CH_2OH of PCL), 3.38 (s, CH_3O), 3.03 (m, CH_2-triazole), 2.92 (s, CH_2S), 2.4-2.8 (m, $COCH_2CH_2$-triazole and CH_2CH_2COO), 2.31 (m, CH_2CO of PCL), 2.23 (m, CH_2CH of P*t*BA), 0.6-2.1 (m, CH_3 resulting from CTA, CH_2 of PCL, and CH_2 and CH_3 of P*t*BA). FT-IR (KBr): 3445, 2940, 2868, 1732, 1638, 1459, 1394, 1369, 1261, 1154, 1093, 1023, 956, 907, 846, 803, 750, 695 cm^{-1}.

Synthesis of PEG(PCL)$_2$(PAA)$_2$ miktoarm star

To a solution of 300 mg of S2 star in DCM (20 mL) was added 0.30 mL of trifluoroacetic acid (TFA) under nitrogen, and the mixture was stirred at room temperature for 16 h. The solution was concentrated and precipitated into a large amount of hexane. After vacuum drying, 235 mg of PEG$(PCL)_2(PAA)_2$ star (S3) was obtained.

PEG$(PCL)_2(PAA)_2$ star: ^1H NMR (DMSO-d_6): δ 12.3 (s, COO*H* of PAA), 7.2-8.0 (m, Ph*H* and C*H* of triazole), 4.1-4.5 (m, CH_2O), 3.98 (t, *J* 6.4, CH_2O of PCL), 3.51 (s, CH_2CH_2O of PEG and terminal CH_2OH of PCL), 3.24 (s, CH_3O), 2.96 (s, CH_2S), 2.87 (m, CH_2-triazole), 2.5-2.8 (m, $COCH_2CH_2$-triazole and CH_2CH_2COO), 2.27 (t, *J* 7.2, CH_2CO of PCL), 2.21 (m, CH_2CH of PAA), 0.6-2.1 (m, CH_3 resulting from CTA, CH_2 of PCL, and CH_2 of PAA). FT-IR (KBr): 3504, 2945, 2866, 1724, 1459, 1420, 1397, 1369, 1296, 1245, 1193, 1107, 1046, 961, 841, 732 cm^{-1}.

Formation of self-assembled and DOX-loaded copolymer aggregates

The copolymer aggregates were prepared by a dialysis method. Briefly, S1 (5.0 mg) was dissolved in 1.0 mL of DMSO and stirred for 2 h at room temperature. Then, the polymer solution was added dropwise into 9.0 mL of phosphate buffered saline (PBS, pH 7.4, 50 mM) solution under vigorous stirring. Two hours later, the solution was transferred into dialysis membrane tubing (MWCO 100 kDa) and dialyzed against PBS solution for 24 h to remove the organic solvent. The radius of gyration (R_g), hydrodynamic radius (R_h) and morphology of aggregates were determined by SLS, DLS and TEM, respectively.

In a typical run to fabricate DOX-loaded aggregates, S1 (20.0 mg) and DOX hydrochloride (4.0 mg) were dissolved in 4.0 mL of DMSO, and followed by addition of about 1.2 mg of triethylamine. After stirring at room temperature for 2 h, the mixture was added dropwise to 36.0 mL of PBS solution (pH 7.4, 50 mM). The solution was stirred for an additional 4 h and dialyzed against PBS solution for 24 h (MWCO 10 kDa). The amount of DOX was determined using fluorescence (FLS920) measurements (excitation at 480 nm and emission at 560 nm). On the basis of fluorescence analysis, the drug loading capacity (DLC) of aggregates was calculated as the weight ratio of actual drug to drug-loaded aggregates, and the drug loading efficiency (DLE) of aggregates was calculated as the weight ratio of actual and added drug content.

In vitro drug release from DOX-loaded aggregates

In a typical run, four portions of DOX-loaded S1 aggregates in PBS solution (3.0 mL, pH 7.4) were put into a dialysis bag (MWCO 10 kDa), which were then immersed into 20 mL of (a) PBS solution (50 mM, pH 7.4) with 10 mM DTT or (b) normal PBS solution at 25 or 37 °C. The tubes were subjected to constant shaking at a fixed temperature. At desired time intervals, 3.0 mL of media outside the dialysis bag were taken for fluorescence measurement and 3.0 mL of fresh media were replenished. The amount of DOX released from aggregates was measured by fluorescence measurement (excitation at 480 nm) at room temperature. All release experiments were performed in triplicate, and the results presented are the average data with standard deviations. Other drug release experiments were conducted according to similar procedures.

Table 1 Results for synthesis of PCL macro CTA (B), PCL-*b*-PNIPAM (BC_1), PCL-*b*-P*t*BA (BC_2), $PEG(PCL)_2(PNIPAM)_2$ (S1) and $PEG(PCL)_2(PtBA)_2$ (S2)[a]

run	polymer	M	solvent	T (°C)	t (h)	C/Y[b]	$M_{n,th}$[c]	M_n[d]	PDI[d]	$M_{n,NMR}$[e]
1	PCL_{44}	CL	toluene	90	20	0.837	5380	8000	1.13	5600
2	PCL_{44}-*b*-$PNIPAM_{32}$	NIPAM	dioxane	70	18	0.708	9200	11200	1.15	9220
3	PCL_{44}-*b*-P*t*BA_{50}	*t*BA	dioxane	70	18	0.803	11800	13100	1.12	12000
4	S1	—	DMF	60	30	0.848	20800	22000	1.08	20900
5	S2	—	DMF	60	30	0.867	26300	27500	1.09	26600

[a] Reaction conditions: $[CL]_0:[HCP]_0:[Sn(Oct)_2]_0$ = 50:1:0.2, $[M]_0$ = 3.0 mol L^{-1} (run 1); $[M]_0:[PCL]_0:[AIBN]_0$ = 45:1:0.1 (run 2) or 60:1:0.1 (run 3), $[M]_0$ = 1.0 mol L^{-1} (runs 2 and 3); $[BC]_0:[PEG\text{-}(N_3)_2]_0:[CuBr]_0:[PMDETA]_0$ = 3:1:2:2, $W_{polymer}:V_{DMF}$ = 0.10 g mL^{-1} (runs 4 and 5). [b] Monomer conversion (C, runs 1-3) and yield (Y, runs 4 and 5) determined by gravimetry or ^1H NMR. [c] Theoretically calculated molecular weight. [d] Number-average molecular weight estimated by GPC ($M_{n,GPC}$, runs 1-3) or determined by GPC-MALLS ($M_{n,LS}$, runs 4 and 5). [e] Number-average molecular weight determined by ^1H NMR analysis.

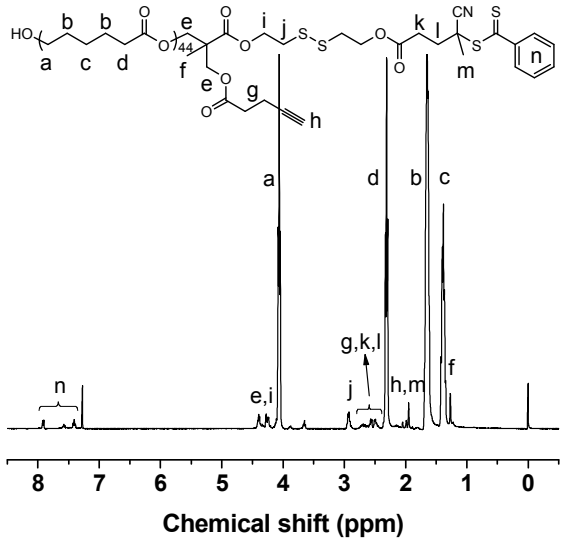

Fig 1. ^1H NMR spectrum of PCL macro CTA.

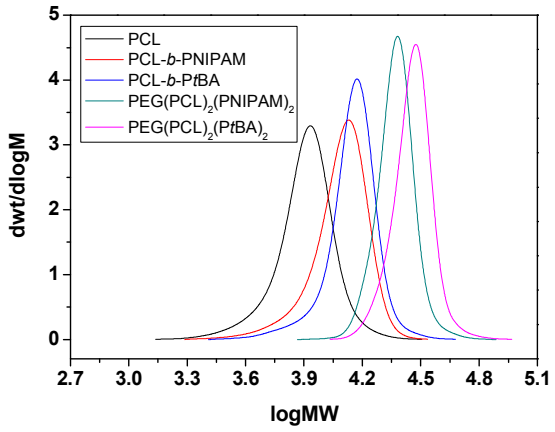

Fig 2. GPC traces of AB_2C_2 star copolymers and their precursors.

Characterization

Apparent molecular weight ($M_{n,GPC}$) and polydispersity (PDI) of linear polymers were measured on a Waters 150-C gel permeation chromatography (GPC) using three Ultrastyragel columns (pore size 50, 100, and 1000 nm, with molecular weight ranges of 100−10000, 500−30000, and 5000−600000 g mol^{-1}, respectively) with 10 μm bead size at 35 °C. THF was used as an eluent at a flow rate of 1.0 mL min^{-1}, and the samples were calibrated with PMMA standard samples. GPC with multiple angle laser scattering detection (GPC-MALLS) was used to determine the absolute number-average molecular weight ($M_{n,LS}$) and polydispersity of star copolymers. GPC was conducted in THF at 35 °C with a flow rate of 1.0 mL min^{-1}. Three TSK-GEL H-type columns (pore size 15, 30 and 200 Å, with molecular weight range of 100–1000, 300–20000 and 5000–400000 g mol^{-1}, respectively) with 5 μm bead size were used. Detection consisted of a RI detector (Optilab rEX) and a multi-angle (14-145°) laser light scattering (MALLS) detector (DAWN HELEOS) with the He-Ne light wave length at 658.0 nm. The refractive index increment d*n*/d*c* for samples were measured off-line by Optilab rEX refractive index detector (λ = 658 nm) at 25 °C using a series of different concentration solutions. Data were collected and processed by use of ASTRA software from Wyatt Technology, and molecular weights were determined by the triple detection method. ^1H (400 MHz) and ^{13}C (100 MHz) spectra were recorded on a Varian spectrometer at 25 °C using $CDCl_3$ or DMSO-d_6 as a solvent. Fourier Transform Infrared (FT-IR) spectra were recorded on a Perkin-Elmer 2000 spectrometer using KBr discs. C, H, N and S were determined by combustion followed by chromatographic separation and thermal conductivity detection using a Carlo-Erba EA 1110CHNO-S Elemental Analyzer. Dynamic light scattering (DLS) measurements were carried out at 25 °C using Zetasizer Nano-ZS from Malvern Instruments equipped with a 633 nm He–Ne laser using back-scattering detection, and the micellar solutions were filtered through a 450 nm syringe filter before measurements. Static light scattering (SLS) measurements over a scattering angle ranging from 30 to 90° were performed at 25 °C on laser light scattering spectrometer

(Brookhaven Inc) equipped with a BI-200SM Goniometer and a BI-TurboCorr digital correlator, and a 22.5 mW red helium-neon laser head operating at 632.8 nm was used as the light source. Fluorescence spectroscopy was recorded at 25 °C on a FLS920 fluorescence spectrometer. Transmission electron microscopy (TEM) images were obtained through a Hitachi H-600 electron microscope.

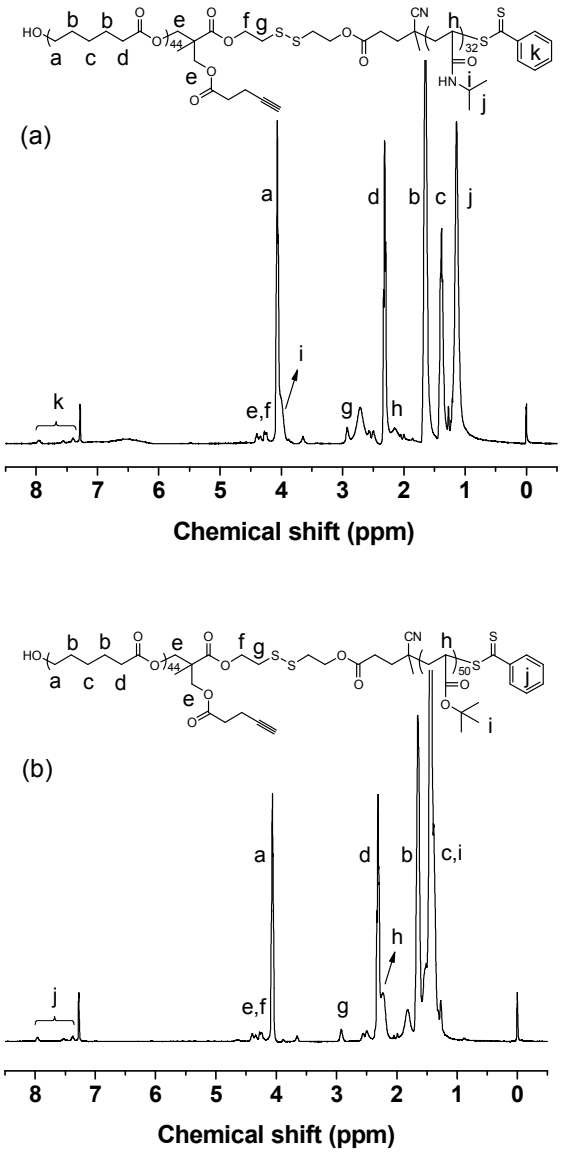

Fig. 3 ^{1}H NMR spectra of alkyne-functionalized PCL-*b*-PNIPAM (a) and PCL-*b*-P*t*BA (b) diblock copolymers.

Results and discussion

Synthesis of AB_2C_2 star terpolymers and their precursors

First, a multifunctional agent 2-((2-((2-hydroxymethyl-2-(pent-4-ynoyloxy)methyl)propionyloxy)ethyl)disulfanyl)ethyl 4-cyano-4-(phenylcarbonothioylthio)pentanoate (HCP) was synthesized by three step reactions. Esterification between 2-((2-hydroxyethyl)disulfanyl)ethyl 4-cyano-4-(phenylcarbonothioylthio)pentanoate (HECP) and isopropylidene-2,2'-bis(methoxyl) propionic acid gave 2-((2-(isopropylidene-2,2'-bis(methoxyl) propionyloxy)ethyl)disulfanyl)ethyl 4-cyano-4-(phenylcarbonothioylthio)pentanoate in 94.6% yield, and followed by deprotection using 1 M HCl in mixtures of water and THF to afford 2-((2-((2,2-dihydroxymethyl)propionyloxy)ethyl)disulfanyl)ethyl 4-cyano-4-(phenylcarbonothioylthio)pentanoate (DCP) in 97.1% yield. On this basis, a selective esterification between DCP and 4-pentynoic acid was performed to afford HCP in 54.6% yield. The chemical structures of HCP and its precursors were confirmed by ^{1}H and ^{13}C NMR, IR, and elemental analysis.

Second, alkyne and disulfide functionalized PCL_{44}-*b*-$PNIPAM_{32}$ (BC_1) and PCL_{44}-*b*-P*t*BA_{50} (BC_2) diblock copolymers were synthesized by successive ROP and RAFT polymerization (Table 1). HCP was used as a functional initiator to perform ROP of CL, and PCL (B) with well-controlled molecular weight and relatively low polydispersity was obtained. In ^{1}H NMR spectrum of PCL (Fig. 1), characteristic resonance signals originated from HCP initiator appeared at 7.92, 7.58, 7.41 (Ph*H*), 2.92 (CH_2S), and 1.99 ppm (C*H*≡C), and resonance signals of PCL segment appeared at 4.06 (CH_2O), 2.31 (CH_2CO), 1.65, and 1.38 ppm (other CH_2). By comparing integration areas at 2.31 (CH_2CO) and 2.92 ppm (CH_2S), the number-average molecular weight determined by ^{1}H NMR ($M_{n,NMR}$) was determined to be 5600 g mol^{-1}, which agreed well with theoretically calculated value ($M_{n,th}$ = 5380 g mol^{-1}). Apparent molecular weight and polydispersity were estimated to be $M_{n,GPC}$ = 8000 g mol^{-1} and PDI = 1.13 by GPC analysis (Fig. 2). PCL was then used as a macro CTA to mediate RAFT polymerization of NIPAM and *t*BA, and BC diblock copolymers were obtained. In ^{1}H NMR spectra (Fig. 3), typical resonance signals of PNIPAM block were noted at 4.01 (C*H*NH), 2.15 (CH_2CH), and 1.14 ppm (CH_3), and resonance signals of P*t*BA block appeared at 2.23 (CH_2CH) and 1.44 ppm (CH_3). On this basis, the $M_{n,NMR}$ values were determined by comparing integration areas of characteristic protons of CH_2S (2.92 ppm) and CH_3 (1.14 ppm for PNIPAM, and 1.44 ppm for P*t*BA). The $M_{n,NMR}$ and $M_{n,th}$ values were similar, and the polydispersity indices were relatively low (PDI = 1.12-1.15), with GPC traces wholly shifted to higher molecular weight side (Fig. 2), revealing the chain extension polymerization was highly efficient performed.

Third, 5-arm AB_2C_2 (A = PEG, B = PCL, and C = PNIPAM or P*t*BA) star copolymers were synthesized by CuAAC reactions. PEG-$(N_3)_2$ and excess BC copolymers were subjected to click reaction in DMF at 60 °C for 30 h, and then excess Si-N_3 and Si-alkyne were added and the reaction was further performed at 80 °C for 20 h. After filtration, concentration and precipitation, the desired star copolymers PEG$(PCL)_2(PNIPAM)_2$ (S1) and PEG$(PCL)_2(PtBA)_2$ (S2) were isolated in 85-87% yield. In ^{1}H NMR spectra of AB_2C_2 stars (Fig. 4), characteristic resonance signals were noted at about 7.5 (C*H*=C of 1,2,3-triazole ring), 3.0 (CH_2 beside 1,2,3-triazole ring), 3.65 (CH_2CH_2O of PEG), 3.38 (terminal CH_3 of PEG), 4.06 (CH_2O of PCL), 2.31 (CH_2CO of PCL), 4.01 (C*H*N of PNIPAM), 2.15 (CH_2CH of PNIPAM), 1.14 (CH_3 of PNIPAM), 2.23 (CH_2CH of P*t*BA), and 1.44 ppm (CH_3 of P*t*BA). The chemical composition was determined to be PEG_{45}-PCL_{90}-$PNIPAM_{63}$ (expected value: PEG_{45}-PCL_{88}-$PNIPAM_{64}$) and PEG_{45}-PCL_{89}-P*t*BA_{101} (expected value: PEG_{45}-

PCL_{88}-P*t*BA_{100}) by ^{1}H NMR analysis, which was in good accordance with the theoretical values by assuming two azide moieties of PEG-$(N_3)_2$ had quantitatively participated in the click reaction. Number-average molecular weight determined by GPC-MALLS ($M_{n,LS}$), $M_{n,NMR}$, and $M_{n,th}$ values were roughly comparable. The isolated star copolymers exhibited monomodal molecular weight distribution, and their GPC traces completely shifted towards higher molecular weight side than their precursors, with polydispersity indices lower than 1.1 (Fig. 2). In IR spectra (b and c of Fig. 5), the characteristic peaks of azide at 2113 cm^{-1} (PEG-$(N_3)_2$, Fig. 5a) wholly disappeared, and the absorbance peaks of various segments were noted at around 1725-1732 ($\nu_{C=O}$ of P*t*BA and PCL), 1648 ($\nu_{C=O}$ of PNIPAM), and 1093 cm^{-1} (ν_{C-O} of PEG).

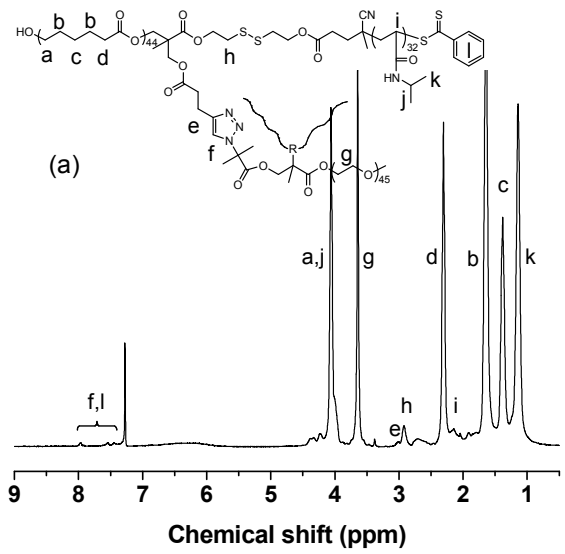

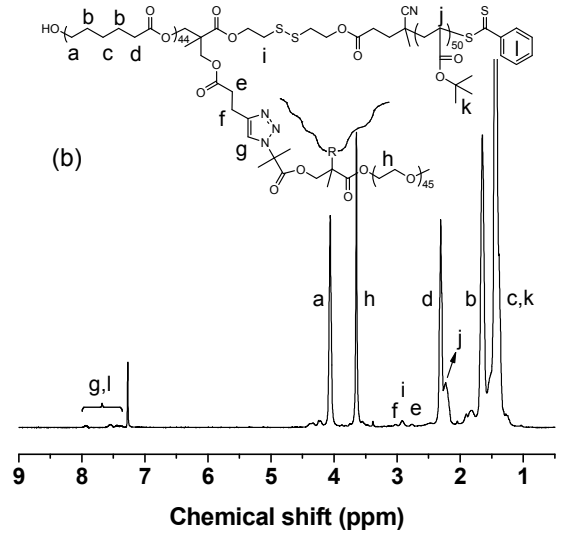

Fig. 4 ^{1}H NMR spectra of PEG$(PCL)_2(PNIPAM)_2$ (a) and PEG$(PCL)_2(PtBA)_2$ (b) star copolymers.

Last, P*t*BA segment of S2 was converted into hydrophilic poly(acrylic acid) (PAA) segment via hydrolysis using trifluoroacetic acid, and PEG$(PCL)_2(PAA)_2$ star (S3) was obtained. Characteristic resonance signals appeared at 12.3 (COO*H* of PAA), 3.98 (CH_2O of PCL), 2.27 (CH_2CO of PCL), 2.21 (CH_2CH of PAA), and 3.51 ppm (CH_2CH_2O of PEG) in ^{1}H NMR spectrum using DMSO-d_6 as a solvent (Fig. S5). The ratios of integration areas of resonance signals in different segments before and after hydrolysis were similar, revealing lack of notable degradation of PCL segments during hydrolysis. The absorbance peaks appeared at 1724 ($\nu_{C=O}$ of PAA and PCL) and 1107 cm^{-1} (ν_{C-O} of PEG) in IR spectrum (Fig. 5d). These results confirmed that the target S3 star was successfully generated by hydrolysis of S2 in dichloromethane.

The above-mentioned results indicated that the modular synthesis and hydrolysis could efficiently afford well-defined star terpolymers with desired chemical composition and controlled molecular weight.

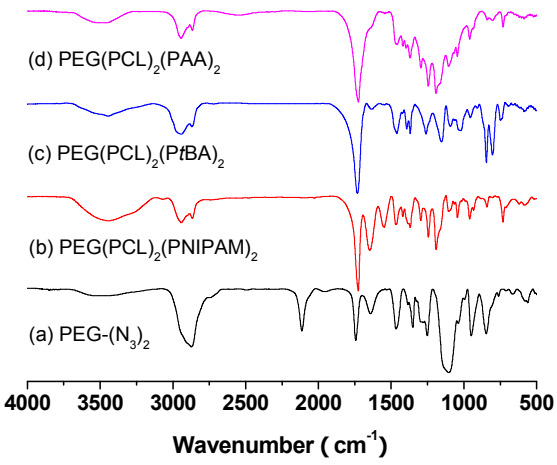

Fig. 5 IR spectra of PEG-$(N_3)_2$ (a) and various AB_2C_2 stars (b-d).

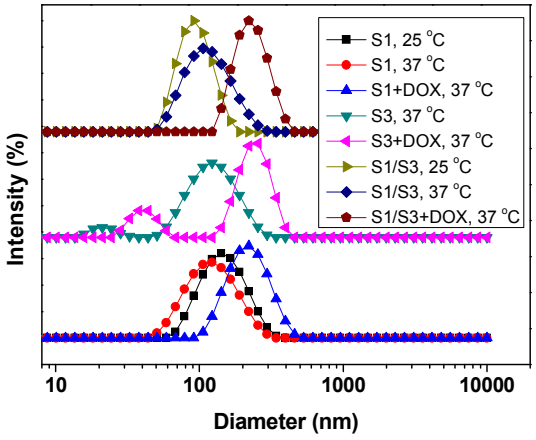

Fig. 6 DLS plots of blank and DOX-loaded copolymer aggregates (c = 0.50 mg mL^{-1}) in PBS solution (pH 7.4, 50 mM) at 25 or 37 °C, in which R_h and PD of aggregates at 25 °C were 64.1 nm, 0.186 (S1), and 43.3 nm, 0.078 (S1/S3).

Formation of copolymer aggregates

Amphiphilic $PEG(PCL)_2(PNIPAM)_2$ (S1), $PEG(PCL)_2(PAA)_2$ (S3) and their mixtures with equimolar ratio (S1/S3) were subjected to self-assembly in aqueous solution (Table 2). For various copolymer aggregates, the average hydrodynamic radius (R_h), peak radius (R_{peak}) and particle size distribution (PD) were determined by DLS (Fig. 6), and the radius of gyration (R_g) was measured by static light scattering (SLS). S1 aggregates exhibited monomodal distribution in DLS plots, and their particle parameters (R_h, R_{peak}, and PD) were obtained as 64.1 nm, 76.6 nm, 0.186 at 25 °C, and 55.6 nm, 64.4 nm, 0.131 at 37 °C. Owing to the enhanced hydrophobic contents at higher temperature, S1 aggregates varied from coexistence of normal and large compound micelles (Fig. S6a, T = 25 °C) to aggregates similar to multicompartment micelles (b and c of Fig. S6, T = 37 °C). S3 aggregates showed bimodal distribution with peak radii at 10.9 and 65.2 nm in DLS plots, and their R_h and PD values were 48.2 nm and 0.241, respectively. As equimolar ratio of S1 and S3 were subjected to coassembly in aqueous solution, comicelles (R_h = 43.3 nm, PD = 0.078, T = 25 °C) and covesicles (R_h = 60.5 nm, PD = 0.126, T = 37 °C) were formed. The R_g/R_h values of various aggregates were 0.754 (S1, 25 °C), 0.853 (S1, 37 °C), 0.747 (S3, 37 °C), 0.760 (S1/S3, 25 °C), and 0.993 (S1/S3, 37 °C), respectively. TEM images (Fig. S6) further confirmed the copolymers were liable to form vesicles (S1/S3, 37 °C) and micelles (other cases) in aqueous solution. The sizes of copolymer aggregates estimated by TEM and DLS were roughly comparable except S1/S3 coaggregates obtained at 37 °C (Fig. S6f), in which the radius (R_h = 60.5 nm) given by DLS was larger than that obtained by TEM image ($R \approx 30$ nm) due to the significant shrinkage of the hollow structures in the dry state. It was found that all the blank aggregates were stable enough at 25 or 37 °C, and no notable precipitation of aggregates was noted in 48 h. After storing for 48 h, monomodal distribution remained in DLS plots of S1/S3 coaggregates, and their R_h and PD values (40.6 nm and 0.102 at 25 °C, and 63.8 nm and 0.134 at 37 °C) were close to the original values (Fig. S7). These results revealed the high stability of coaggregates in the absence of external stimuli.

Dually and triply stimuli-triggered drug release from DOX-loaded copolymer aggregates

The drug release properties were strongly dependent on polymeric architectures, and the star copolymer aggregates usually exhibited more controllable release behaviors than linear copolymer micelles. In this study, thermo-responsive PNIPAM and pH-sensitive PAA segments were introduced in disulfide-bearing 5-arm AB_2C_2 stars to construct dual-responsive systems. Taking account into the enhanced difficulty to synthesize multiple stimuli-responsive star quaterpolymers such as PEG-$(PCL)_2$-PNIPAM-PAA star, the mixture of S1 and S3 stars according to equimolar ratio was used as an alternative copolymer sensitive to thermo, pH and reduction stimuli. In theory, the coaggregates formed by star mixtures can exhibit versatile stimuli-triggered properties owing to adjustable feed ratio, and thus they are expected to possess a great potential in multifunctional drug delivery systems.

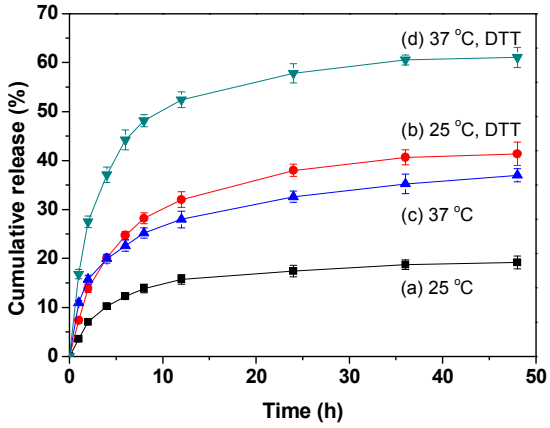

Fig. 7 In vitro drug release profiles of DOX-loaded reduction- and thermo-sensitive S1 aggregates (c = 0.50 mg mL^{-1}) in PBS solution (50 mM) with or without 10 mM DTT at 25 or 37 °C.

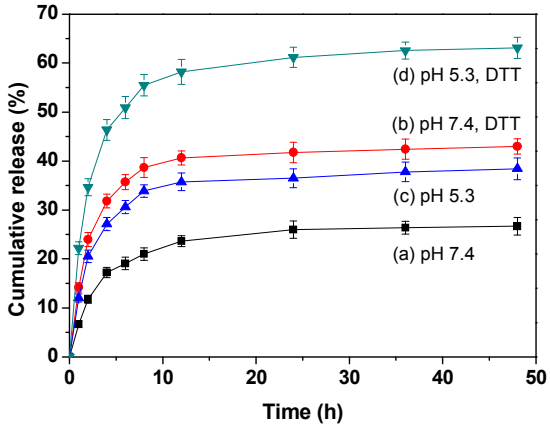

Fig. 8 In vitro drug release profiles of DOX-loaded reduction- and pH-sensitive S3 micelles (c = 0.50 mg mL^{-1}) in PBS solution (50 mM) with or without 10 mM DTT at 37 °C.

DOX was selected as a model hydrophobic drug to determine the drug release properties upon external stimuli. The drug was encapsulated into copolymer aggregates at 37 °C by dialysis method, and the hydrodynamic diameters of DOX-loaded copolymer aggregates were significantly larger than those of blank aggregates (Table 2). The drug loading capacity (DLC) and drug loading efficiency (DLE) of DOX-loaded copolymer aggregates were determined by fluorescence analysis. Their DLC and DLE values of various aggregates were determined to be within 4.63-7.72% (for DLC) and 23.2-38.6% (for DLE). The DLC and DLE values of S3 micelles and S1/S3 coaggregates were very close, and both were higher than those S1 micelles. On this basis, the thermo-, pH- and reduction-triggered drug release properties of DOX-loaded copolymer aggregates were investigated in detail (Table S1).

The in vitro drug releases from thermo- and reduction-sensitive S1 aggregates were performed in PBS solution (pH 7.4, 50 mM) with or without 10 mM DTT at predetermined temperature (T =

Table 2 Influence of composition on properties of copolymer aggregates at 37 °C

sample	R_g (nm)[a]	R_h (nm)[a]	PD[a]	R_{peak} (nm)[a]	R_g/R_h	R_h (nm)[b]	PD[b]	R_{peak} (nm)[b]	DLC (%)	DLE (%)
S1	47.4	55.6	0.131	64.4	0.853	100	0.213	114	4.63	23.2
S3	36.0	48.2	0.241	10.9, 65.2[c]	0.747	118	0.515	20.7, 122[c]	7.72	38.6
S1/S3	60.1	60.5	0.126	60.2	0.993	119	0.192	118	7.29	36.5

[a] Radius of gyration (R_g), hydrodynamic radius (R_h), particle size distribution (PD), and peak radius (R_{peak}) of blank aggregates obtained by SLS and DLS analyses. [b] R_h, PD and R_{peak} values of DOX-loaded copolymer aggregates. [c] Bimodal distribution was observed.

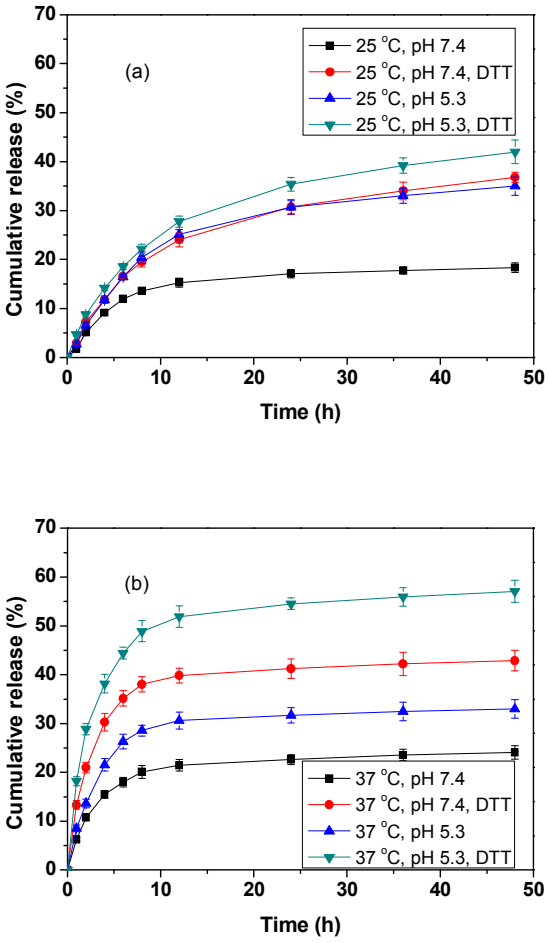

Fig. 9 In vitro drug release profiles of DOX-loaded S1 and S3 coaggregates (c = 0.50 mg mL^{-1}) in PBS solution (50 mM) upon external stimuli.

25 or 37 °C) for 48 h. The maximum release rate under different conditions was liable to decrease in the order 37 °C + DTT > 37 °C > 25 °C + DTT > 25 °C, in which the apparent release rate (K) derived from the release profiles was in the range of 0.0291-0.161 h^{-1} (Fig. 7). Although the initial release rate at 37 °C without DTT was faster than that at 25 °C using 10 mM DTT, the former exhibited smaller release amount when the time was beyond 4 h due to reduced release rate. The cumulative release amount at 48 h was 19.2% (25 °C), 41.4% (25 °C + DTT), 37.0% (37 °C), and 61.1% (37 °C + DTT), corresponding to the increment of cumulative release (ICR, defined as the enhanced percent as compared with the lowest cumulative release amount) of 116% (25 °C + DTT), 93% (37 °C), and 218% (37 °C + DTT) under different stimuli. The release rate of DOX from S1 micelles at 37 °C was significantly enhanced than that at 25 °C, and the release kinetics could be further accelerated as reduction stimulus (10 mM DTT) was applied, corresponding to dually stimuli-triggered release properties of S1 aggregates. In addition to enhanced solubility of DOX in water at higher temperature, the destabilization of copolymer micelles induced by increased hydrophobicity of PNIPAM segment above low critical solution temperature (LCST) could account for the faster release kinetics at 37 °C. As different amount of reducing agent and various temperatures were used, the release kinetics of DOX-loaded S1 aggregates could be theoretically adjusted in a wide range due to the gradual change in microenvironment.

Similarly, the in vitro drug releases of DOX from pH- and reduction-responsive S3 micelles were performed in PBS solution (pH 7.4 or 5.0, 50 mM) with or without 10 mM DTT at 37 °C. The release rate under different conditions (K = 0.065-0.215 h^{-1}) tended to reduce in the order pH 5.3 + DTT > pH 7.4 + DTT > pH 5.3 > pH 7.4, and only limited encapsulated drug could be efficiently released from copolymer micelles when the time was beyond 12 h (Fig. 8). The cumulative release amount at 48 h was 26.7% (pH 7.4), 43.0% (pH 7.4 + DTT), 38.4% (pH 5.3) and 63.1% (pH 5.3 + DTT), respectively. The faster release rate of DOX under acidic conditions could be partly ascribed to the increased solubility of DOX and the weakened electrostatic interaction between PAA and drug. When 10 mM DTT was applied, the disulfide linkages could be cleaved, resulting in the formation of PEG(PCL)$_2$ star and PAA chains. The change in microenvironment caused the variation in strength of hydrogen-bonding interactions, van der Waals forces and electrostatic repulsions, which further affected the interactions among the drug, copolymer and release media and thus resulted in faster release of DOX. Owing to the synergistic effect of acid and reduction stimuli, the cumulative release from S3 micelles upon dual stimuli (pH 5.3 and 10 mM DTT) was 136% higher than that at pH 7.4 without DTT. In theory, the release properties of DOX-loaded S3 aggregates could be adjusted by changing pH value and amount of reducing agent.

Moreover, the in vitro drug releases of DOX from triply responsive S1 and S3 mixed aggregates were also investigated. The drug release behaviors in PBS solution normally exhibited release profiles similar to triple phases, which roughly involved a fast release rate within the initial stage up to 2-3 h, a moderate

release rate within a second period up to 8-12 h, and a slow release rate with extended time (Fig. 9). As different stimuli were added, the apparent release rate (K, h^{-1}) derived from the first stage was decreased in the order 37 °C + pH 5.3 + DTT (0.177), 37 °C + pH 7.4 + DTT (0.135), 37 °C + pH 5.3 (0.0837), 37 °C + pH 7.4 (0.0618), 25 °C + pH 5.3 + DTT (0.496), 25 °C + pH 7.4 + DTT (0.0393), 25 °C + pH 5.3 (0.0326), 25 °C + pH 7.4 (0.0261), which revealed the release kinetics of DOX-loaded coaggregates could be adjusted by choosing suitable stimuli. Lack of external stimuli (25 °C + pH 7.4), the cumulative release amount at 48 h was 18.3%. When external stimuli were applied, the cumulative release amount at 48 h was in the range of 24.1%-57.1%, corresponding to ICR values within 32%-212%. The coaggregates formed from S1 and S3 mixtures were stable enough during DOX loading and release. Meanwhile, the external stimuli such as temperature, pH and amount of reducing agent could be freely changed, and thus the stimuli-triggered release kinetics was potentially adjusted in a wide range on demand.

Therefore, normal S1 and S3 micelles enabled dually stimuli-triggered release processes, while the coaggregates formed from S1 and S3 stars could be efficiently used for construction of triply responsive systems for smart drug delivery. Since multiple reactions are necessary to synthesize star and block copolymers with enhanced chemical compositions, this straightforward strategy via coaggregation of copolymer mixtures with suitable interactions may be more promising to fabricate multiply sensitive aggregates. In addition to utilization of different types of external stimuli, the release process can be potentially adjusted by changing the feed ratio of star mixtures owing to the influence of segment composition on secondary interactions. Fabrication and properties of triply responsive coaggregates with different ratios of star terpolymers are under way.

Conclusions

Novel $PEG(PCL)_2(PNIPAM)_2$ (S1) and $PEG(PCL)_2(PAA)_2$ (S3) star terpolymers were synthesized by modular synthesis, and the drug release properties of copolymer aggregates upon thermo, pH and reduction stimuli were investigated. The resultant miktoarm star copolymers possessed well-controlled molecular weight, low polydispersity and precise composition, evident from ^{1}H NMR and GPC-MALLS analyses. In the presence of external stimuli, remarkably enhanced release kinetics was noted, and the maximum increment of cumulative release from various aggregates at 48 h could reach up to 218% (S1 micelles), 136% (S3 micelles), and 212% (mixed aggregates). These stimuli-sensitive copolymer aggregates had a great potential in smart drug delivery due to their reasonable drug loading efficiency and stimuli-adjustable release properties. The mixed aggregates may be more promising due to their versatile release properties relative to external multiple stimuli and composition of star mixtures. Our study paves ways for facile construction of triply sensitive drug release systems via versatile coaggregation, which can be extended to generate other types of multiply responsive aggregates formed by complex macromolecular architecture and their mixtures.

Acknowledgements

This work was financially supported by the National Natural Science Foundation of China (Grants 21074081 and 21274096), and the Project Funded by the Priority Academic Program Development of Jiangsu Higher Education Institutions.

Notes and references

Jiangsu Key Laboratory of Advanced Functional Polymer Design and Application, Department of Polymer Science and Engineering, College of Chemistry, Chemical Engineering and Materials Science, Soochow University, Suzhou 215123, China. Tel: +86-512-65882045; Fax: +86-512-65882045; E-mail: ylzhao@suda.edu.cn

† Electronic Supplementary Information (ESI) available: [IR and ^{1}H NMR spectra, TEM images, and DLS plots]. See DOI: 10.1039/b000000x/

1 R. K. O'Reilly, C. J. Hawker and K. L. Wooley, *Chem. Soc. Rev.*, 2006, **35**, 1068–1083.
2 J. Z. Du and R. K. O'Reilly, *Soft Matter*, 2009, **5**, 3544–3561.
3 M. Motornov, Y. Roiter, I. Tokarev and S. Minko, *Prog. Polym. Sci.*, 2010, **35**, 174–211.
4 A. E. Smith, X. W. Xu and C. L. McCormick, *Prog. Polym. Sci.*, 2010, **35**, 45–93.
5 D. Roy, J. N. Cambre and B. S. Sumerlin, *Prog. Polym. Sci.*, 2010, **35**, 278–301.
6 Y. F. Zhou, W. Huang, J. Y. Liu, X. Y. Zhu and D. Y. Yan, *Adv. Mater.*, 2010, **22**, 4567–4590.
7 H. Y. Tian, Z. H. Tang, X. L. Zhuang, X. S. Chen and X. B. Jing, *Prog. Polym. Sci.*, 2012, **37**, 237–280.
8 A. E. Felber, M.-H. Dufresne and J.-C. Leroux, *Adv. Drug Delivery Rev.*, 2012, **64**, 979–992.
9 E. Fleige, M. A. Quadir and R. Haag, *Adv. Drug Delivery Rev.*, 2012, **64**, 866–884.
10 H. B. Jin, W. Huang, X. Y. Zhu, Y. F. Zhou and D. Y. Yan, *Chem. Soc. Rev.*, 2012, **41**, 5986–5997.
11 J. M. Hu, G. Q. Zhang and S. Y. Liu, *Chem. Soc. Rev.*, 2012, **41**, 5933–5949.
12 X. Z. Yan, F. Wang, B. Zheng and F. H. Huang, *Chem. Soc. Rev.*, 2012, **41**, 6042–6065.
13 J. F. Gohy and Y. Zhao, *Chem. Soc. Rev.*, 2013, **42**, 7117–7129.
14 F. D. Jochum and P. Theato, *Chem. Soc. Rev.*, 2013, **42**, 7468–7483.
15 J. M. Zhuang, M. R. Gordon, J. Ventura, L. Y. Li and S. Thayumanavan, *Chem. Soc. Rev.*, 2013, **42**, 7421–7435.
16 J. Nicolas, S. Mura, D. Brambilla, N. Mackiewicz and P. Couvreur, *Chem. Soc. Rev.*, 2013, **42**, 1147–1235.
17 R. Cheng, F. H. Meng, C. Deng, H. A. Klok and Z. Y. Zhong, *Biomaterials*, 2013, **34**, 3647–3657.
18 W. Hua, R. X. Zhuo and X. Z. Zhang, *Prog. Polym. Sci*., 2013, **38**, 503–535.
19 Z. Y. Qiao, R. Zhang, F. S. Du, D. H. Liang and Z. C. Li, *J. Controlled Release*, 2011, **152**, 57–66.
20 W. Chen, P. Zhong, F. H. Meng, R. Cheng, C. Deng, J. Feijen and Z. Y. Zhong, *J. Controlled Release*, 2013, **169**, 171–179.
21 Y. D. Gu, Y. N. Zhong, F. H. Meng, R. Cheng, C. Deng and Z. Y. Zhong, *Biomacromolecules*, 2013, **14**, 2772–2780.
22 J. Dai, S. D. Lin, D. Cheng, S. Y. Zou and X. T. Shuai, *Angew. Chem., Int. Ed.*, 2011, **50**, 9404–9408.
23 Y. Wang, C. Y. Hong and C. Y. Pan, *Biomacromolecules*, 2013, **14**, 1444–1451.
24 W. Shao, K. Miao, H. H. Liu, C. N. Ye, J. Z. Du and Y. L. Zhao, *Polym. Chem.*, 2013, **4**, 3398–3410.
25 K. Miao, W. Shao, H. H. Liu and Y. L. Zhao, *Polym. Chem*., 2014, **5**, 1191–1201.
26 X. L. Hu, J. Tian, T. Liu, G. Y. Zhang and S. Y. Liu, *Macromolecules*, 2013, **46**, 6243−6256.
27 A. Klaikherd, C. Nagamani and S. Thayumanavan, *J. Am. Chem. Soc.*, 2009, **131**, 4830–4838.
28 P. Bilalis, A. Chatzipavlidis, L. A. Tziveleka, N. Boukos and G. Kordas, *J. Mater. Chem.*, 2012, **22**, 13451–13454.
29 O. Bertrand, C. A. Fustin and J. F. Gohy, *ACS Macro Lett.*, 2012, **1**, 949–953.

30 P. Schattling, F. D. Jochum and P. Theato, *Chem. Commun.*, 2011, **47**, 8859–8861.
31 Y. Y. Mai and A. Eisenberg, *Chem. Soc. Rev.*, 2012, **41**, 5969–5985.
32 G. S. Chen and M. Jiang, *Chem. Soc. Rev*., 2011, **40**, 2254–2266.
33 Y. Zhao, F. Sakai, L. Su, Y. J. Liu, K. C. Wei, G. S. Chen and M. Jiang, *Adv. Mater*., 2013, **25**, 5215–5256.
34 Y. F. Zhou and D. Y. Yan, *Chem. Commun.*, 2009, 1172–1188.
35 S. Groger, D. Geschke, J. Karger, F. Stallmach and C. Konak, *Macromol. Rapid Commun*., 2004, 25, 1015–1018.
36 Y. Xiao, J. Wu, J. S. Kin and A. Eisenberg, *Langmuir*, 2006, **22**, 419–424.
37 D. V. Pergushov, I. A. Babin, F. A. Plamper, A. B. Zezin and A. H. E. Müller, *Langmuir*, 2008, **24**, 6414–6419.
38 M. Xiong, Y. M. Chen and M. Maskos, *Macromol. Rapid Commun*., 2008, **29**, 1368–1371.
39 N. Lefèvre, C.-A. Fustin and J.-F. Gohy, *Macromol. Rapid Commun.,* 2009, **30**, 1871–1888.
40 S. G. Yang, X. F. Yu, L. Wang, Y. F. Tu, J. X. Zheng, J. T. Xu, R. M. Van Horn and S. Z. D. Cheng, *Macromolecules*, 2010, **43**, 3018–3026.
41 A. B. E. Attia, Z. Y. Ong, J. L. Hedrick, P. P. Lee, P. L. R. Ee, P. T. Hammond and Y. Y. Yang, *Curr. Opin. Colloid Inter. Sci*., 2011, **16**, 182–194.
42 X. J. Huang, Y. Xiao and M. D. Lang, *J. Colloid Inter. Sci*., 2011, **364**, 92–99.
43 C. Y. Wang, S. G. Yang, X. F. Yu, J. X. Zheng, J. H. Ma, J. Xua and M. F. Zhu, *Soft Matter*, 2012, **8**, 10307–10313.
44 V. Ladmiral, M. Semsarilar, I. Canton and S. P. Armes, *J. Am. Chem. Soc.*, 2013, **135**, 13574–13581.
45 Z. B. Li, E. Kesselman, Y. Talmon, M. A. Hillmyer and T. P. Lodge, *Science,* 2004, **306**, 98−101.
46 Z. B. Li, M. A. Hillmyer and T. P. Lodge, *Macromolecules,* 2004, **37**, 8933−8940.
47 T. P. Lodge, A. Rasdal, Z. B. Li and M. A. Hillmyer, *J. Am. Chem. Soc.,* 2005, **127**, 17608−17609.
48 Z. B. Li, M. A. Hillmyer and T. P. Lodge, *Nano Lett.,* 2006, **6**, 1245−1249.
49 Z. B. Li, M. A. Hillmyer and T. P. Lodge, *Macromolecules,* 2006, **39**, 765−771.
50 A. O. Moughton, M. A. Hillmyer and T. P. Lodge, *Macromolecules,* 2012, **45**, 2−19.
51 S. Junnila, N. Houbenov, S. Hanski, H. Iatrou, A. Hirao, N. Hadjichristidis and O. Ikkala, *Macromolecules,* 2010, **43**, 9071−9076.
52 S. Junnila, N. Houbenov, A. Karatzas, N. Hadjichristidis, A. Hirao, H. Iatrou and O. Ikkala, *Macromolecules,* 2012, **45**, 2850–2856.
53 A. H. Groschel, F. H. Schacher, H. Schmalz, O. V. Borisov, E. B. Zhulina, A. Walther and A. H. E. Müller, *Nat. Commun*., 2012, **3**, 710.
54 Y. L. Zhao, T. Higashihara, K. Sugiyama and A. Hirao, *J. Am. Chem. Soc.,* 2005, **127**, 14158–14159.
55 C. N. Ye, G. D. Zhao, M. J. Zhang, J. Z. Du and Y. L. Zhao, *Macromolecules*, 2012, **45**, 7429−7439.
56 P. F. Gou, W. P. Zhu and Z. Q. Shen, *Biomacromolecules*, 2010, **11**, 934–943.
57 L. Y. Li, W. D. He, J. Li, B. Y. Zhang, T. T. Pan, X. L. Sun and Z. L. Ding, *Biomacromolecules*, 2010, **11**, 1882–1890.
58 H. Y. Cho, A. Srinivasan, J. Hong, E. Hsu, S. G. Liu, A. Shrivats, D. Kwak, A. K. Bohaty, H. J. Paik, J. O. Hollinger and K. Matyjaszewski, *Biomacromolecules*, 2011, **12**, 3478–3486.
59 H. T. Duong, C. P. Marquis, M. Whittaker, T. P. Davis and C. Boyer, *Macromolecules*, 2011, **44**, 8008–8019.
60 X. J. Li, Y. F. Qian, T. Liu, X. L. Hu, G. Y. Zhang, Y. Z. You and S. Y. Liu, *Biomaterials*, 2011, **32**, 6595–6605.
61 G. M. Soliman, A. Sharma, D. Maysinger and A. Kakkar, *Chem. Commun.*, 2011, **47**, 9572–9587.
62 D. Cameron and M. P. Shaver, *Chem. Soc. Rev.*, 2011, **40**, 1761–1776.
63 K. Fukae, T. Terashima and M. Sawamoto, *Macromolecules*, 2012, **45**, 3377–3386.
64 J. N. Liu, H. Duong, M. R. Whittaker, T. P. Davis and C. Boyer, *Macromol. Rapid Commun.*, 2012, **33**, 760–766.
65 X. Liu, Z. C. Tian, C. Chen and H. R. Allcock, *Polym. Chem.*, 2013, **4**, 1115–1125.
66 H. Y. Cho, S. E. Averick, E. Paredes, K. Wegner, A. Averick, S. Jurga, S. R. Das and K. Matyjaszewski, *Biomacromolecules*, 2013, **14**, 1262–1267.
67 H. C. Kolb, M. G. Finn and K. B. Sharpless, *Angew. Chem., Int. Ed*., 2001, **40**, 2004−2021.
68 Y. Mitsukami, M. S. Donovan, A. B. Lowe and C. L. McCormick, *Macromolecules,* 2001, **34**, 2248−2256.
69 L. Tao, J. Q. Liu, G. H. Tan and T. P. Davis, *Macromolecules*, 2009, **42**, 4960−4962.
70 P. Wu, M. Malkoch, J. N. Hunt, R. Vestberg, E. Kaltgrad, M. G. Finn, V. V. Fokin, K. B. Sharpless and C. J. Hawker, *Chem. Commun.*, 2005, 5775–5777.
71 Y. K. Huang, T. T. Hou, X. Q. Cao, S. Perrier and Y. L. Zhao, *Polym. Chem*., 2010, **1**, 1615–1623.
72 G. D. Zhao, P. P. Zhang, C. B. Zhang and Y. L. Zhao, *Polym. Chem.,* 2012, **3**, 1803–1812.

Graphical Abstract:

Thermo, pH and reduction responsive coaggregates comprising AB_2C_2 star terpolymers for multi-triggered release of doxorubicin

Ke Miao, Huanhuan Liu and Youliang Zhao

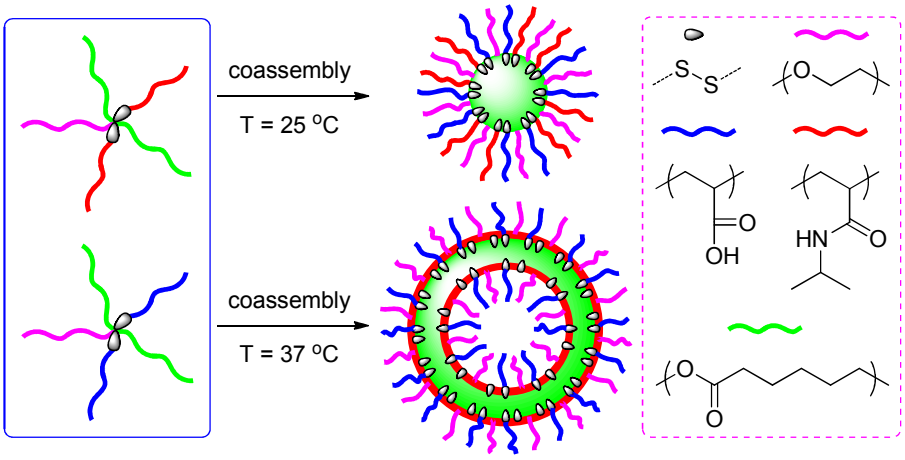

Novel disulfide-linked $PEG(PCL)_2(PNIPAM)_2$ and $PEG(PCL)_2(PAA)_2$ star terpolymers were synthesized and coassembled into mixed micelles or vesicles for multi-triggered drug release.